Summer solstice orchestrates the subcontinental-scale synchrony of mast seeding

—

Valentin Journé[1], Jakub Szymkowiak[1,2], Jessie Foest[3], Andrew Hacket-Pain[3], Dave Kelly[4], Michał Bogdziewicz*[1]

[1]Forest Biology Center, Institute of Environmental Biology, Faculty of Biology, Adam Mickiewicz University, Uniwersytetu Poznańskiego 6, 61-614 Poznan, Poland.
[2]Population Ecology Research Unit, Institute of Environmental Biology, Faculty of Biology, Adam Mickiewicz University, Uniwersytetu Poznańskiego 6, 61-614 Poznan, Poland.
[3]Department of Geography and Planning, School of Environmental Sciences, University of Liverpool, Liverpool, United Kingdom.
[4]Centre for Integrative Ecology, School of Biological Sciences, University of Canterbury, Christchurch, New Zealand

*corresponding author: michalbogdziewicz@gmail.com

High interannual variation in seed production in perennial plants, can be synchronized at subcontinental scales with wide consequences for ecosystem functioning, but how such synchrony is generated is unclear. We investigated the factors contributing to masting synchrony in European beech (*Fagus sylvatica*), that extends to the 2000 km geographic range. Maximizing masting synchrony via spatial weather coordination, known as the Moran effect, requires a simultaneous response to weather conditions across distant populations. A celestial cue that occurs simultaneously across the entire Hemisphere is the longest day (summer solstice). We show that European beech abruptly opens its temperature-sensing window on the solstice, hence widely separated populations all start responding to weather signals in the same week. This celestial "starting gun" generates ecological events with high spatial synchrony across the continent.

Introduction

Subcontinental synchronization of interannual variation in seed production by trees means that, in a large-seeding year, a large pulse of resources is made available to wildlife over the majority of the continent by virtue of the synchronous reproduction by millions of trees [1–3]. Such large-seeding years are usually followed by reproductive failures, creating subsequent famine [4, 5]. This synchronized cycle of abundance and shortage triggers far-reaching disruptions in food webs, including rodent outbreaks [6], migration of ungulates and birds [7–11], and spikes in wildlife-borne human diseases [12, 13]. Moreover, in some species tree and leaf growth is reduced in years of high seed production, creating large-scale fluctuations in carbon sequestration [14–16]. The spatial scale of synchrony is a key aspect that amplifies the ecological importance of year-to-year variation in seed production [17–19]. However, several key questions on how plants synchronize masting over such extensive spatial scales remain unanswered.

Masting is synchronous and highly variable reproduction among years by a population of perennial plants [20]. Synchrony often exceeds among populations and decades of investigation have demonstrated that the regional synchronization of masting stems from the Moran effect, i.e. it is driven by spatially synchronized environmental signals [1, 2, 7, 21–25]. A major mechanism that governs the annual allocation of resources to seed production is weather variation [26–28]. These so-called weather cues are employed by plants to maintain synchronized reproductive fluctuations within populations [29]. The mechanisms underpinning weather cues exhibit species-specific variation, with a major example being the influence of summer temperature on the promotion of flower production [30, 31]. Masting plants have evolved to be remarkably responsive to temperature fluctuations [29, 32]. Consequently, substantial flowering effort, or masting, is triggered when the temperature meets some species-specific criteria. For example, one common link is that warm summers are associated with a high subsequent seed crop [33–36]. If individuals and populations collectively respond to the same cue across extensive regions, the spatial scale of masting synchrony aligns with the broad-scale synchronization of weather patterns [2, 21, 23, 24]. Crucially, the highest regional synchrony is achieved if the cue window is temporally conserved [3]. For instance, if the cue window shifts among populations to be earlier in the year in warmer climates, akin to the advancement of bud break or flowering in warmer climate [37, 38], regional synchrony deteriorates [3].

A global comparison of the Moran effect in masting showed that European beech (*Fagus sylvatica*) has stronger spatial synchrony than any other species in Europe (matched only by white spruce, *Picea glauca*, in North America). Both species have very large ranges, including latitudinally (north-south), which makes their ability to maintain significant masting synchrony exceeding 1500 km especially puzzling [2, 3]. New evidence has demonstrated that the timing of the cue window is exceptionally well conserved across the range of European beech [3], but the mechanism facilitating this stability remains unknown.

Recently, Zohner *et al.* [39] showed that temperature has opposite effects on leaf senes-

cence phenology before and after the summer solstice, demonstrating that trees can time their physiology using maximum day length. Similarly, wood formation in trees switches from a focus on cell division to secondary wall thickening once days start to shorten [40, 41]. The capacity to sense the timing of solstice might explain the remarkable consistency of the temporal window during which beech trees are receptive to cues triggering masting events [3, 42]. Right across the European continent, the cues are anchored to June and July temperatures despite great differences in climate and day length among studied sites (mean summer annual temperature range across sites: 7.7 – 16.6 ℃, maximum day length 15 hr 25 mins to 16 hr 50 mins) [3], and a significant warming trend (1℃ over 40 years) [42], resulting in substantial variation in the growing season onset and duration. Here, we show that European beech achieves high synchrony across very large scales by anchoring the weather cue window to the summer solstice - the longest day of the year that occurs simultaneously across the whole Northern Hemisphere. The solstice alignment enables cohesive timekeeping across distant beech populations inhabiting diverse climatic regions.

Results

Weather cues in beech are anchored to the solstice

We used a moving window analysis and observed an abrupt rise in the correlation between European beech seed production and temperatures at the summer solstice, showing that the longest day coincides with the opening of the cue window. We ran a moving window correlation between annual seed production and mean temperatures in 61 populations of European beech sampled across the species' range (Fig. 1a, mean number of annual observations per site = 35, max = 68), across which masting synchrony reaches 2000 km (Fig. 1b). The correlation coefficients displayed two distinct peaks, consistent among populations independent of latitude or local climate (Fig. 1c). The first was a negative peak occurring two years before seed fall, and the second was a positive peak arising one year before seed fall, both following the summer solstice (Fig. 1c). The correlations' directions between European beech masting and temperature in the summers before seed fall, one (T1), and two (T2) years prior align with previous research [33, 42, 44]. Here, however, we discover that the June-July period is not a mere consequence of physiological processes operating at that time in the plant (such as resource priming in year T2; cf. [44]), but the cue anchoring to the solstice. According to our hypothesis, European beech uses the solstice as a trigger to open the cue window. In support of this, correlation coefficient values between seed production and temperature rapidly increased after the solstice, compared to before it (Fig. 2). To test that, we fitted a generalized additive model (GAM), in which a response was the correlation between annual seed production and mean temperature in the 7-day rolling window. The predictors were relative day length (with maximum happening at the summer solstice) and the summer solstice as a categorical variable (before and after the solstice)

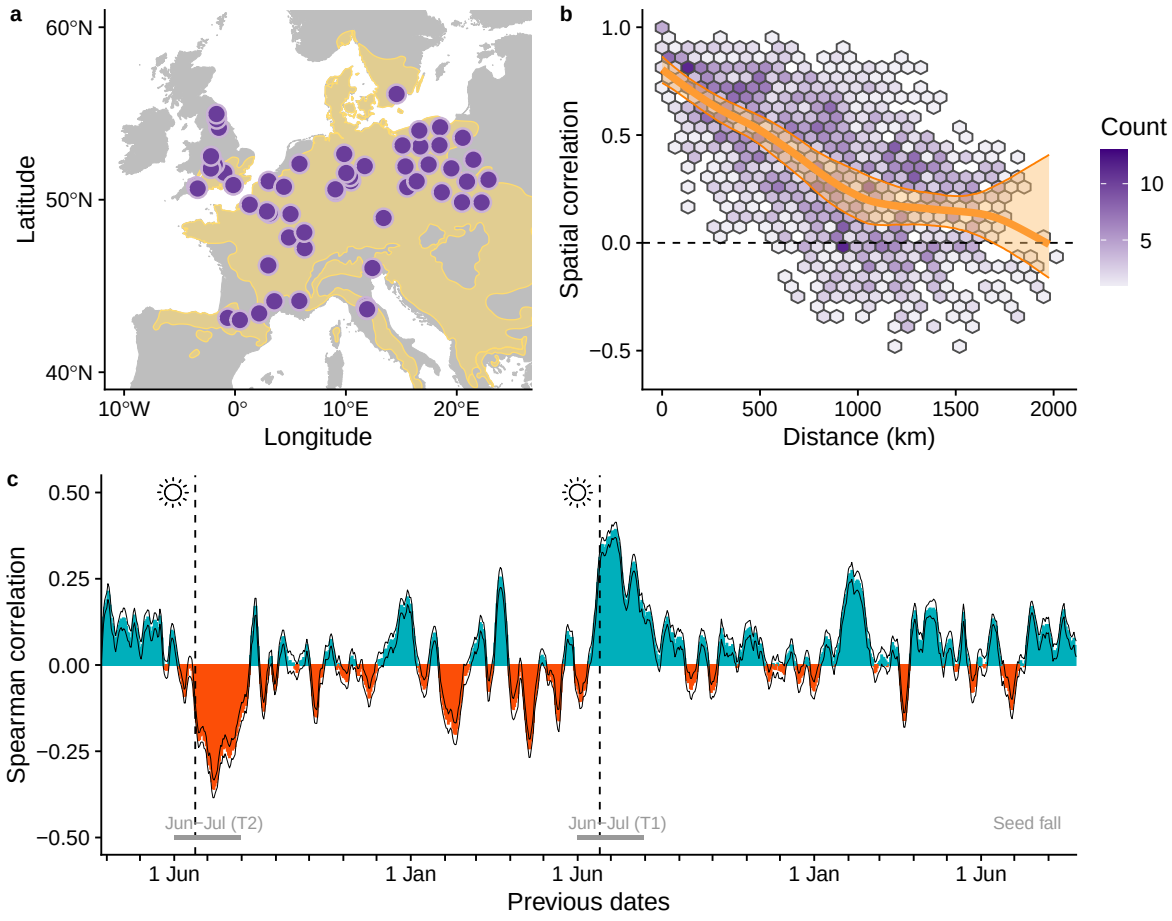

Figure 1: a) Locations of the 61 time series of annual seed production of European beech used in the study (average N years per series = 38). The yellow area highlights the species range (based on EUFORGEN, [43]). b) Spatial correlation between seed production over years and sites. The orange line represents the non-parametric spatial covariance function, with the shaded area showing 95% bootstrap confidence envelope. Hexes are pairwise Spearman correlations between sites, with the hex color scaled to the number of observations within each hex. Pairwise correlations were calculated for series with at least 5 years of overlap, that we deemed a minimum number of observations to calculate a correlation. c) Mean rolling Spearman correlation between temperature and masting averaged across all 61 sites. The graph shows correlations in two (T2) and one (T1) years before seed production, up until September when seed fall happens. The size of the temperature window is 7 days, with a 1-day step, and correlations are plotted according to the day of the year at the end of each 7-day window. Black dashed lines close to the sun icon indicate the summer solstice (21st June). Correlations are coded blue for positive, and red for negative. The black solid lines represent the standard error of the correlation coefficients across the sites for each window. Correlation for each site separately is reported in Fig S1.

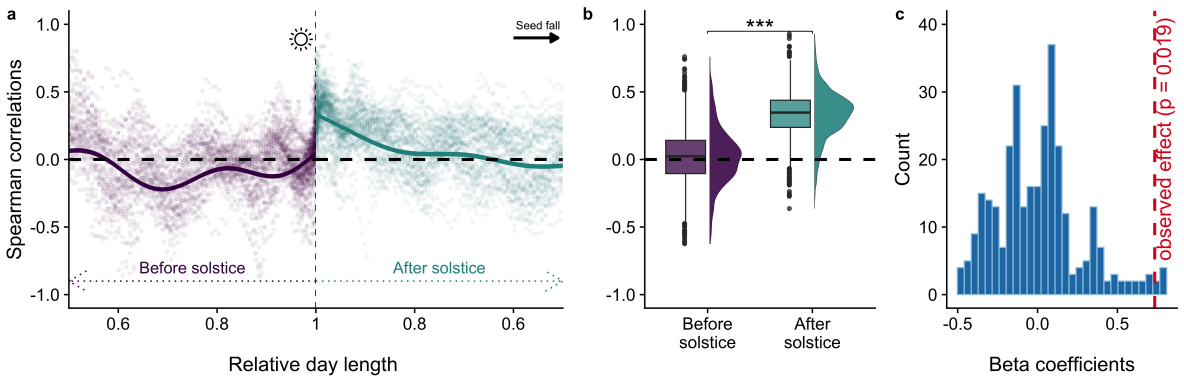

Figure 2: a) Correlations between European beech seed production and temperature at 7-day windows abruptly increase just after the summer solstice. The prediction lines and associated 95% confidence intervals are based on the GAM model with Spearman correlation coefficients as a response and interaction between relative day length (at the particular time window) and the time of the year (before vs. after the summer solstice (as a categorical variable) as predictors. Each point is the per site (N =61) per window correlation coefficient. b) Correlations shown at before and after the solstice shown at a) binned into 0.95 - 1 (max) day length before and after the solstice to help visualize abrupt change at the same day length at the two sides of the solstice. The asterisks indicate a significant ($p<0.0001$) difference between boxplots (see Methods). c) Results of a null model testing whether the abrupt increase in the correlation coefficients (between masting and summer temperatures) is highest at the summer solstice or any other day in the year. Histogram shows the distribution of beta coefficients under the null hypothesis i.e. the before-after difference in correlation coefficients in any other day of the year considered instead of the solstice. The red dashed line shows the observed effect i.e., how correlation coefficients "after solstice" differ as compared to "before solstice". The null model was rejected ($p = 0.02$). All three graphs show the effects for summer T1 (one year before seedfall), effects for summer T2 are presented in Fig. S2.

with their interaction. The interaction was significant (Table S1), showing that European beech abruptly starts responding to temperature after, but not before, the solstice. The predicted correlation between masting and temperature was ~4-fold higher one day after the solstice compared to one day before (correlation before the solstice, 0.095; after the solstice, 0.37, Fig. 2). Comparing the correlations in bins, defined as 0.95 - 1 (max) day length, before (mean correlation = 0.02) and after the solstice (0.35) shows an even greater magnitude of difference (Fig. 2b). We rejected the null hypothesis that the highest difference in correlations at the solstice would emerge by chance ($p = 0.02$) (Fig. 2c) (see Methods for details). Similar anchoring at solstice was observed for the temperature effects in year T2 (Fig. S2).

Discussion

More than a mere outcome of the Moran effect, the regional synchrony in European beech masting stems from a mechanism that effectively harnesses weather variation for synchro-

nization. The negative correlation of European beech masting with temperatures in summer T2 has been proximally associated with enhanced resource accumulation in cooler years [44, 45], and the positive correlation in summer T1 with enhanced flower primordia differentiation [30, 33, 44]. Of course, the positive effect of resource accumulation on seed production does not only appear after the longest day, and flower primordia can begin differentiating in response to high temperatures before the celestial event. Theoretical predictions suggest that masting can be triggered by any weather cue, yet cues are most likely to evolve from weather variation that affects reproduction-related processes [20, 29, 46]. This sensitivity of such reproduction-related physiological processes is then reinforced by natural selection when variable and synchronized reproduction enhances plant fitness, as documented in a previous study on European beech [47]. However, to ensure ecological synchrony through weather-based alignment, cue-sensing phenology must be harmonized across populations. In species in which the cue-sensing is not harmonized, such as *Picea abies* or *Quercus robur*, synchrony deteriorates [3]. Temperatures are highly synchronized across space, but not necessarily over time. If one population opens its weather cue window in July, but another in August, they will likely be responding to different temperature conditions, and their subsequent masting patterns will diverge, reducing synchrony [3]. The problem is that plants at more northern latitudes have much longer days (by more than an hour) near midsummer than plants further south, so using absolute day length to open the weather cue window would result in a spread of cue windows by latitude, and consequently large-scale asynchrony. A celestial cue that happens simultaneously across the entire continent, capable of transcending environmental diversity among very distant populations is the annual maximum day length at the summer solstice. European beech responds to the solstice to open the cue window on the same day at all latitudes, which creates a high precision timing of the Moran effect.

In addition to summer temperatures, beech masting is correlated with summer (June/July) precipitation (in T1 and T2), and with spring weather [16, 44]. We thus run a similar, 7-days moving window analysis for precipitation. Consistent with past work, precipitation in June and July was positively (in T2) and negatively (in T1) correlated with seed production (Fig. S3. That effect was, however, not anchored to the solstice. Based on that, we hypothesize that temperature is the primary weather cue for beech masting, while precipitation during these periods may modulate the strength of temperature effects. That is supported by generally weaker and less spatially consistent correlations between beech masting and precipitation compared to temperature effects reported in past studies [44, 48]. Analyses based on gene expression levels will shed more light on these mechanisms. The effects of weather during pollination appear generally negligible compared to summer weather [44], even if important locally [16]. In support, the peaks in correlations during the flowering season are not distinguishable from fluctuations along the two-year period that precedes seed fall (Fig. 1, S3).

The observation that seed production in European beech is highly correlated with temperatures around the solstice reinforces the theory that weather cues can serve as a prox-

imate mechanism enabling masting plants to synchronize patterns of seed production at supra-annual and regional scales. The pivotal role of weather variation in driving seed production in masting plants is not controversial [32]. However, the precise translation of weather variation into seed production variability remains a topic of debate [29, 49–51]. On one hand, weather conditions may influence the transition from flowers to fruits by, for example, disrupting pollination success or hindering resource uptake [45, 52, 53]. On the other hand, gene regulatory networks might integrate various signals, such as temperature and photoperiod, allowing flowering to occur only when all these cues are received [54]. In the latter scenario, hormones and genes that control flowering exhibit hypersensitivity to environmental signals, thus granting masting a degree of independence from resource- and pollen-related mechanisms [29]. The fact that European beech responsiveness to temperature is prominent only as the days begin to shorten suggests that weather's influence on masting extends beyond mere effects on flower development stages. Rather, it implies the presence of a strongly conserved regulatory network that enables all plants to respond uniformly to the cue. Future research should involve monitoring gene expression levels, such as the FLOWERING LOCUS T, at the fine temporal scales disclosed in this study, to understand how the negative (two years before seed fall, T2) and positive (in year T1) correlations with temperature are translated into genetic and hormonal processes [30, 31, 55, 56].

Across the entire continent, the summer solstice serves as a celestial "starting gun" that enables cohesive timekeeping across far-distant beech populations, highlighting how evolution may have capitalized on this astronomical event to maximize ecological synchrony. A prime fitness benefit of masting lies in predator satiation [20, 32]. The synchronized, substantial year-to-year variation in seed production effectively starves seed consumers in low-seeding years, making it easier to satiate these consumer populations in mast years [57]. High regional synchrony of masting appears to have a selective advantage as it allows to satiate mobile seed consumers, such as highly mobile vertebrates [9, 18], that can prevent regeneration if mast years are localized [58]. Large-scale synchrony also increases the likelihood of seed release into disturbed areas [18]. Variation in day length provides a reliable signal of seasonal shifts and is unaffected by climatic changes in space and time [59]. To increase masting synchrony under the Moran effect, populations separated by hundreds of kilometers align their cue window with the moment when day length reaches its longest duration once a year.

Anchoring to solstice means that the timing of cue sensing withstands climate variation and generates a high scale of regional synchrony. However, the climate changes of the twenty-first century generate novel challenges that may prove the solstice-anchoring suboptimal. In European beech, increasing temperatures lead to a decrease in interannual variation and synchrony of seed production, a process called masting breakdown [60]. The consequence is inefficient predator satiation and decreased pollination efficiency that together lead to a collapse in viable seed production [61]. The breakdown follows from higher summer temperatures and therefore more frequent triggering of reproduction [42]. If sum-

mer cues would not be anchored to the solstice, shifting the sensitive periods to earlier in the season would perhaps compensate for the change in cueing frequency. Second, climate change leads not only to trends in mean weather conditions but also to changes in large-scale weather patterns [62]. Long-lasting blocking weather patterns that create extreme conditions over certain regions, appear to change in frequency [62]. For example, high-pressure areas sandwiched between low-pressure systems called an omega block, can bring long-lasting heat to the high-pressure area [62, 63]. Transition probabilities towards omega in summer over the Northern Hemisphere increase over time, which may create repeated periods of masting asynchrony between low- and high-pressure blocks. Similarly, the among-site variation in correlation values between temperatures and masting could be associated with omega blocking. The consequences of such disruptions in the large-scale patterns of synchrony appear as an interesting avenue for future research.

Recent discovery indicated that solstice triggers a shift in trees' responsiveness to temperature, enabling plants to anticipate the approaching end of the growing season [39]. Our study shows that the solstice also serves as a continent-wide "starting gun" to which plants respond simultaneously from southern France to Sweden, and orchestrates the multiyear-long process that determines reproductive investment in European beech, generating ecological events marked by the unparalleled spatial synchrony across the continent.

Data availability statement

The data used in this study have been deposited in the Open Science Framework (OSF) (DOI: 10.17605/OSF.IO/S2CD4). The full MASTREE+ dataset is available in [64]. Climate data have been extracted from E-OBS at https://cds.climate.copernicus.eu/cdsapp#!/dataset/insitu-gridded-observations-europe?tab=form.

Code availability statement

R statistical software v4.3.0 was used in this work [65]. All analyses used published R packages.

Acknowledgements

This study was supported by the European Union (ERC, ForestFuture, 101039066). Views and opinions expressed are however those of the authors only and do not necessarily reflect those of the European Union or the European Research Council. Neither the European Union nor the granting authority can be held responsible for them. VJ was supported by project No. 2021/43/P/NZ8/01209 co-funded by the Polish National Science Centre and the EU H2020 research and innovation programme under the MSCA GA No. 945339. For the purpose of Open Access, the author has applied a CC-BY public copyright licence to any Author Accepted Manuscript (AAM) version arising from this submission.

Author Contributions Statement

MB conceived the study, MB, VJ, JSz, JF, AHP, DK designed the study. VJ and JSz performed the analysis, MB led the writing of the manuscript. All authors contributed critically to the interpretation of the analysis and drafts, and gave final approval for publication.

Competing Interests Statement

None declared.

Materials and Methods

Study system and data European beech (*Fagus sylvatica* L.) is a major forest-forming species in temperate Europe. Beech is a model masting species, with seed production characterized by large interannual variation and synchrony of seed production [16, 22, 66]. Beech masting allows to escape seed predation and increases pollination efficiency [60, 66]. Subsequent cold (two years before seed fall) and hot (one year before seed fall) summers trigger large seed production in European beech [33, 44].

Seed production and environmental data Annual observations of seed production of European beech were extracted from MASTREE+, an open-access database of annual records of population-level reproductive effort [64]. For our analysis, we restricted the European beech time series to the continuous observations of seed production that covered more than 14 years, observed after 1952. We excluded pollen-based and ordinal records. We used a conservative, relatively high number of years per time series, to ensure that enough mast years had a chance to happen and optimize the signal-to-noise ratio. The cut-off in 1952 was motivated by limited climatic data availability before that year. That resulted in 61 time series available for the analysis (averaged length time series, 35 years; maximum length time series, 68 years). The number of years per time series is given in Fig. S1. We extracted daily climate data for each site from the corresponding 0.1 ° grid cell of the E-OBS dataset [67].

The day length for each location was calculated as

$$\cos \omega_0 = -\tan(\frac{\phi \times \pi}{180}) \times \tan \delta \tag{1}$$

where ω_0 is the solar hour angle, ϕ is latitude and δ is declination. Declination of the sun can be obtained with

$$\delta = \frac{\pi \times 23.45}{180} \times \sin(\frac{2 \times \pi \times (284 + \mathrm{DOY})}{365}) \tag{2}$$

where DOY is Day of the Year. Day length in hours was obtained with

$$\mathrm{DL} = \begin{cases} 0 & \omega_0 > 1 \\ 24 & \omega_0 < -1 \\ \frac{24}{\pi \times \mathrm{acos}(\omega_0)} & \text{otherwise} \end{cases} \tag{3}$$

For each site, the relative day length was normalized to the 0 - 1 range.

Moving window correlation To determine how correlations between mast seeding and temperature fluctuate at a fine temporal scale, we ran a moving window correlation analysis. Specifically, we ran a moving Spearman correlation between log-transformed annual seed

production and mean daily temperature. The window size was set as 7 days, with a 1-day step. The moving window size was set relatively small to ensure the detection of fine-scale temporal changes in the correlation between masting and temperature. Correlations were run over year T2 (two years before seed fall) and T1 (one year before seed fall), as we expected the June-July summer cues [33, 44] to be fine-tuned to the summer solstice. Moving window correlations were run for each site separately. We computed the standard error of the Spearman correlation (cor_{se}) as

$$cor_{se} = \sqrt{(1 - cor^2)^2 \times \frac{(1 + cor^2/2)}{(n - 3)}} \quad (4)$$

with cor being the estimated Spearman correlation value and n the sample size [68].

Cue window and the solstice To test whether the change in Spearman correlations between masting and temperature changes abruptly at solstice we used generalized additive models (GAM). We included the correlation coefficients as a response, while the relative day length, the summer solstice as a categorical variable (before or after the solstice), and their interaction were used as predictors. If the cue window opens at the solstice, we expected the interaction to be significant, with the correlation abruptly increasing at the solstice. We fitted GAMs with a beta distribution family, by using the `mgcv` package (v1.8-42, [69]), and specified the restricted maximum likelihood (REML) method to estimate smoothing parameters. We fitted models using the beta distribution because fitting a model with a Gaussian distribution of errors, given our response type, would have been inappropriate and result in biased parameter estimates. Because the beta distribution requires the response to be bounded between 0 and 1, we rescaled the Spearman correlations to 0-1 range. The scaling was done for each site separately and is a simple mathematical transformation that does not affect the distribution of a variable. We used the inverse of the standard error of correlation coefficients (i.e. $1/cor_{se}$) as weights in the GAM models, to ensure that observations with higher error had lower weight on parameter estimates [70]. The site was included as a random intercept. We tested for spatial autocorrelation of model residuals using the `DHARMa` package (v0.4.6) [71], and detected none. The test was run separately for correlations in one (T1) and two (T2) years before seed fall.

As an additional test, we also binned the moving window correlations between masting and temperature changes into two categories, i.e. before and after the solstice. For each bin, we used a number of days that included 5% of change in day length at each side of the solstice (24 days). We tested for the difference between the period (i.e. before/after the solstice) using the GAM model with correlations in these bins as a response, while including group (before/after the solstice) as a predictor fitted as a parametric term.

Furthermore, we used a null model to explicitly test whether the observed increase in the values of correlation coefficients between masting and temperature just after solstice could emerge by chance also if any other day of the year was considered instead of the solstice.

For each day of the year between 25th January and 6th December we compared correlation coefficients for 24 days before and 24 days after that day using analogous GAM models as described above. From these models, we extracted the beta coefficients for the "after" category, showing how correlation coefficients differ as compared to the "before" category. This procedure resulted in a distribution of beta coefficients under the null hypothesis i.e. the before-after difference in correlation coefficients if any other day of the year would have been considered instead of the solstice. Then, to test for the significance of the solstice effect (i.e. whether the increase in the values of correlation coefficients we observed at the solstice is more probable than given purely by chance), we calculated the p-value as the number of times an absolute value of randomized beta coefficients was greater than, or equal to, the absolute value of a beta coefficient from GAM model comparing correlations binned around the solstice, divided by the number of tests.

References

1. Koenig, W. D. & Knops, J. M. Scale of mast-seeding and tree-ring growth. *Nature* **396,** 225–226 (1998).
2. LaMontagne, J. M., Pearse, I. S., Greene, D. F. & Koenig, W. D. Mast seeding patterns are asynchronous at a continental scale. *Nature Plants* **6,** 460–465 (2020).
3. Bogdziewicz, M., Journé, V., Hacket-Pain, A. & Szymkowiak, J. Mechanisms driving interspecific variation in regional synchrony of trees reproduction. *Ecology Letters* **26,** 754–764 (2023).
4. Ostfeld, R. S. & Keesing, F. Pulsed resources and community dynamics of consumers in terrestrial ecosystems. *Trends in Ecology Evolution* **15,** 232–237 (2000).
5. Bogdziewicz, M., Zwolak, R. & Crone, E. E. How do vertebrates respond to mast seeding? *Oikos* **125,** 300–307 (2016).
6. Pucek, Z, Jędrzejewski, W, Jędrzejewska, B & Pucek, M. Rodent population dynamics in a primeval deciduous forest (Białowieża National Park) in relation to weather, seed crop, and predation. *Acta Theriologica* **38,** 199–232 (1993).
7. Jenni, L. Mass Concentrations of Bramblings Fringilla montifringilla in Europe 1900-1983: Their Dependence upon Beech Mast and the Effect of Snow-Cover. *Scandinavian Journal of Ornithology* **18,** 84–94 (1987).
8. Mcshea, W. J. THE INFLUENCE OF ACORN CROPS ON ANNUAL VARIATION IN RODENT AND BIRD POPULATIONS. *Ecology* **81,** 228–238 (2000).
9. Curran, L. M. & Webb, C. O. Experimental Tests of the Spatiotemporal Scale of Seed Predation in Mast-Fruiting Dipterocarpaceae. *Ecological Monographs* **70,** 129 (2000).

10. Koenig, W. D. & Knops, J. M. Seed-crop size and eruptions of North American boreal seed-eating birds. *Journal of Animal Ecology* **70,** 609–620 (2001).

11. Szymkowiak, J. & Thomson, R. L. Nest predator avoidance during habitat selection of a songbird varies with mast peaks and troughs. *Behavioral Ecology and Sociobiology* **73** (2019).

12. Jones, C. G., Ostfeld, R. S., Richard, M. P., Schauber, E. M. & Wolff, J. O. Chain reactions linking acorns to gypsy moth outbreaks and Lyme disease risk. *Science* **279,** 1023–1026 (1998).

13. Bregnard, C., Rais, O. & Voordouw, M. J. Masting by beech trees predicts the risk of Lyme disease. *Parasites and Vectors* **14,** 1–22 (2021).

14. Hacket-Pain, A. J. *et al.* Climatically controlled reproduction drives interannual growth variability in a temperate tree species. *Ecology Letters* **21,** 1833–1844 (2018).

15. Vergotti, M. J., Fernández-Martínez, M., Kefauver, S. C., Janssens, I. A. & Peñuelas, J. Weather and trade-offs between growth and reproduction regulate fruit production in European forests. *Agricultural and Forest Meteorology* **279** (2019).

16. Mund, M. *et al.* It is not just a 'trade-off': indications for sink- and source-limitation to vegetative and regenerative growth in an old-growth beech forest. *New Phytologist* **226,** 111–125 (2020).

17. Koenig, W. D. *et al.* Dissecting components of population-level variation in seed production and the evolution of masting behavior. *Oikos* **102,** 581–591 (2003).

18. Ascoli, D. *et al.* Modes of climate variability bridge proximate and evolutionary mechanisms of masting. *Philosophical Transactions of the Royal Society B: Biological Sciences* **376** (2021).

19. Qiu, T. *et al.* Masting is uncommon in trees that depend on mutualist dispersers in the context of global climate and fertility gradients. *Nature Plants* **9,** 1044–1056 (2023).

20. Kelly, D. The evolutionary ecology of mast seeding. *Trends in Ecology Evolution* **9,** 465–470 (1994).

21. Koenig, W. D. & Knops, J. M. H. Large-scale spatial synchrony and cross-synchrony in acorn production by two California oaks. *Ecology* **94,** 83–93 (2013).

22. Ascoli, D. *et al.* Inter-annual and decadal changes in teleconnections drive continental-scale synchronization of tree reproduction. *Nature Communications* **8,** 1–9 (2017).

23. Wion, A. P., Weisberg, P. J., Pearse, I. S. & Redmond, M. D. Aridity drives spatiotemporal patterns of masting across the latitudinal range of a dryland conifer. *Ecography* **43,** 569–580 (2020).

24. Bogdziewicz, M., Hacket-Pain, A., Ascoli, D. & Szymkowiak, J. Environmental variation drives continental-scale synchrony of European beech reproduction. *Ecology* **102,** e03384 (2021).

25. Reuman, D. C. *et al.* How environmental drivers of spatial synchrony interact. *Ecography* (2023).

26. Abe, T. *et al.* Parameterisation and validation of a resource budget model for masting using spatiotemporal flowering data of individual trees. *Ecology Letters* **19,** 1129–1139 (2016).

27. Schermer, E. *et al.* Flower phenology as a disruptor of the fruiting dynamics in temperate oak species. *New Phytologist* **225,** 1181–1192 (2020).

28. Pesendorfer, M. B. *et al.* The ecology and evolution of synchronized reproduction in long-lived plants. *Philosophical Transactions of the Royal Society B: Biological Sciences* **376,** 20200369 (2021).

29. Kelly, D. *et al.* Of mast and mean: Differential-temperature cue makes mast seeding insensitive to climate change. *Ecology Letters* **16,** 90–98 (2013).

30. Satake, A., Kawatsu, K., Teshima, K., Kabeya, D. & Han, Q. Field transcriptome revealed a novel relationship between nitrate transport and flowering in Japanese beech. *Scientific Reports* **9,** 4325 (2019).

31. Samarth *et al.* Molecular control of the floral transition in the mast seeding plant Celmisia lyallii (Asteraceae). *Molecular Ecology* **30,** 1846–1863 (2021).

32. Pearse, I. S., Koenig, W. D. & Kelly, D. Mechanisms of mast seeding: resources, weather, cues, and selection. *New Phytologist* **212,** 546–562 (2016).

33. Piovesan, G. & Adams, J. M. Masting behaviour in beech: Linking reproduction and climatic variation. *Canadian Journal of Botany* **79,** 1039–1047 (2001).

34. Schauber, E. M. *et al.* MASTING BY EIGHTEEN NEW ZEALAND PLANT SPECIES: THE ROLE OF TEMPERATURE AS A SYNCHRONIZING CUE. *Ecology* **83,** 1214–1225 (2002).

35. Fernández-Martínez, M., Vicca, S., Janssens, I. A., Espelta, J. M. & Peñuelas, J. The North Atlantic Oscillation synchronises fruit production in western European forests. *Ecography* **40,** 864–874 (2017).

36. Nussbaumer, A. *et al.* Impact of weather cues and resource dynamics on mast occurrence in the main forest tree species in Europe. *Forest Ecology and Management* **429,** 336–350 (2018).

37. Fu, Y. H. *et al.* Declining global warming effects on the phenology of spring leaf unfolding. *Nature* **526,** 104–107 (2015).

38. Zohner, C. M., Benito, B. M., Svenning, J. C. & Renner, S. S. Day length unlikely to constrain climate-driven shifts in leaf-out times of northern woody plants. *Nature Climate Change* **6,** 1120–1123 (2016).

39. Zohner, C. M. *et al.* Effect of climate warming on the timing of autumn leaf senescence reverses after the summer solstice. *Science* **381** (2023).

40. Rossi, S. *et al.* Conifers in cold environments synchronize maximum growth rate of tree-ring formation with day length. *New Phytologist* **170,** 301–310 (2006).

41. Luo, T. *et al.* Summer solstice marks a seasonal shift in temperature sensitivity of stem growth and nitrogen-use efficiency in cold-limited forests. *Agricultural and Forest Meteorology* **248,** 469–478 (2018).

42. Bogdziewicz, M. *et al.* Climate warming causes mast seeding to break down by reducing sensitivity to weather cues. *Global Change Biology* **27,** 1952–1961 (2021).

43. Caudullo, G., Welk, E. & San-Miguel-Ayanz, J. Chorological maps for the main European woody species. *Data in Brief* **12,** 662–666 (2017).

44. Vacchiano, G. *et al.* Spatial patterns and broad-scale weather cues of beech mast seeding in Europe. *New Phytologist* **215,** 595–608 (2017).

45. Smaill, S. J., Clinton, P. W., Allen, R. B. & Davis, M. R. Climate cues and resources interact to determine seed production by a masting species. *Journal of Ecology* **99,** 870–877 (2011).

46. Janzen, D. H. Seed predation by animals. *Annual Review of Ecology and Systematics* **2,** 465–492 (1971).

47. Bogdziewicz, M. *et al.* Climate Change Strengthens Selection for Mast Seeding in European Beech. *Current Biology* **30,** 3477–3483.e2 (2020).

48. Drobyshev, I. *et al.* Masting behaviour and dendrochronology of European beech (Fagus sylvatica L.) in southern Sweden. *Forest Ecology and Management* **259,** 2160–2171 (2010).

49. Crone, E. E. & Rapp, J. M. Resource depletion, pollen coupling, and the ecology of mast seeding. *Annals of the New York Academy of Sciences* **1322,** 21–34 (2014).

50. Pearse, I. S., Koenig, W. D. & Knops, J. M. H. Nordic Society Oikos Cues versus proximate drivers: testing the mechanism behind masting behavior. *Oikos* **123,** 179–184 (2014).

51. Fleurot, E. *et al.* Oak masting drivers vary between populations depending on their climatic environments. *Current Biology* **33,** 1117–1124.e4 (2023).

52. Koenig, W. D., Knops, J. M., Carmen, W. J. & Pearse, I. S. What drives masting? The phenological synchrony hypothesis. *Ecology* **96,** 184–192 (2015).

53. Schermer, E. *et al.* Pollen limitation as a main driver of fruiting dynamics in oak populations. *Ecology Letters* **22,** 98–107 (2019).

54. Satake, A. & Kelly, D. Studying the genetic basis of masting. *Philosophical Transactions of the Royal Society B* **376** (2021).

55. Böhlenius, H. *et al.* CO/FT regulatory module controls timing of flowering and seasonal growth cessation in trees. *Science* **312,** 1040–1043 (2006).

56. Miyazaki, Y. *et al.* Nitrogen as a key regulator of flowering in Fagus crenata: understanding the physiological mechanism of masting by gene expression analysis. *Ecology Letters* **17,** 1299–1309 (2014).

57. Zwolak, R., Celebias, P. & Bogdziewicz, M. Global patterns in the predator satiation effect of masting: A meta-analysis. *Proceedings of the National Academy of Sciences of the United States of America* **119,** e2105655119 (2022).

58. Bogdziewicz, M. *et al.* Emerging infectious disease triggered a trophic cascade and enhanced recruitment of a masting tree. *Proceedings of the Royal Society B: Biological Sciences* **289** (2022).

59. Way, D. A. & Montgomery, R. A. Photoperiod constraints on tree phenology, performance and migration in a warming world. *Plant Cell and Environment* **38,** 1725–1736 (2015).

60. Bogdziewicz, M., Kelly, D., Thomas, P. A., Lageard, J. G. A. & Hacket-Pain, A. Climate warming disrupts mast seeding and its fitness benefits in European beech. *Nature Plants* **6,** 88–94 (2020).

61. Bogdziewicz, M. *et al.* Reproductive collapse in European beech results from declining pollination efficiency in large trees. *Global Change Biology* (2023).

62. Detring, C., Müller, A., Schielicke, L., Névir, P. & Rust, H. W. Occurrence and transition probabilities of omega and high-over-low blocking in the Euro-Atlantic region. *Weather and Climate Dynamics* **2,** 927–952 (2021).

63. Woollings, T. *et al.* Blocking and its Response to Climate Change. *Current Climate Change Reports* **4,** 287–300 (2018).

64. Hacket-Pain, A. *et al.* MASTREE+: Time-series of plant reproductive effort from six continents. *Global Change Biology* **28,** 3066–3082 (2022).

65. R Core Team. *R: A Language and Environment for Statistical Computing* (R Foundation for Statistical Computing, Vienna, Austria, 2023).

66. Nilsson, S. G. & Wastljung, U. Seed Predation and Cross-Pollination in Mast-Seeding Beech (Fagus Sylvatica) Patches. *Ecology* **68,** 260–265 (1987).

67. Cornes, R. C., van der Schrier, G., van den Besselaar, E. J. & Jones, P. D. An Ensemble Version of the E-OBS Temperature and Precipitation Data Sets. *Journal of Geophysical Research: Atmospheres* **123,** 9391–9409 (2018).

68. Bonett, D. G. & Wright, T. A. Sample size requirements for estimating Pearson, Kendall and Spearman correlations. *Psychometrika* **65,** 23–28 (2000).

69. Wood, S. *Generalized Additive Models: An Introduction with R* 2nd ed. (Chapman and Hall/CRC, 2017).

70. Zuur, A., Ieno, E., Walker, N. & Saveliev, A. Mixed effects models and extensions in ecology with R. *Springer* **2009th ed.** (2009).

71. Hartig, F. *DHARMa: Residual Diagnostics for Hierarchical (Multi-Level / Mixed) Regression Models* R package version 0.4.6 (2022).

Supplementary material

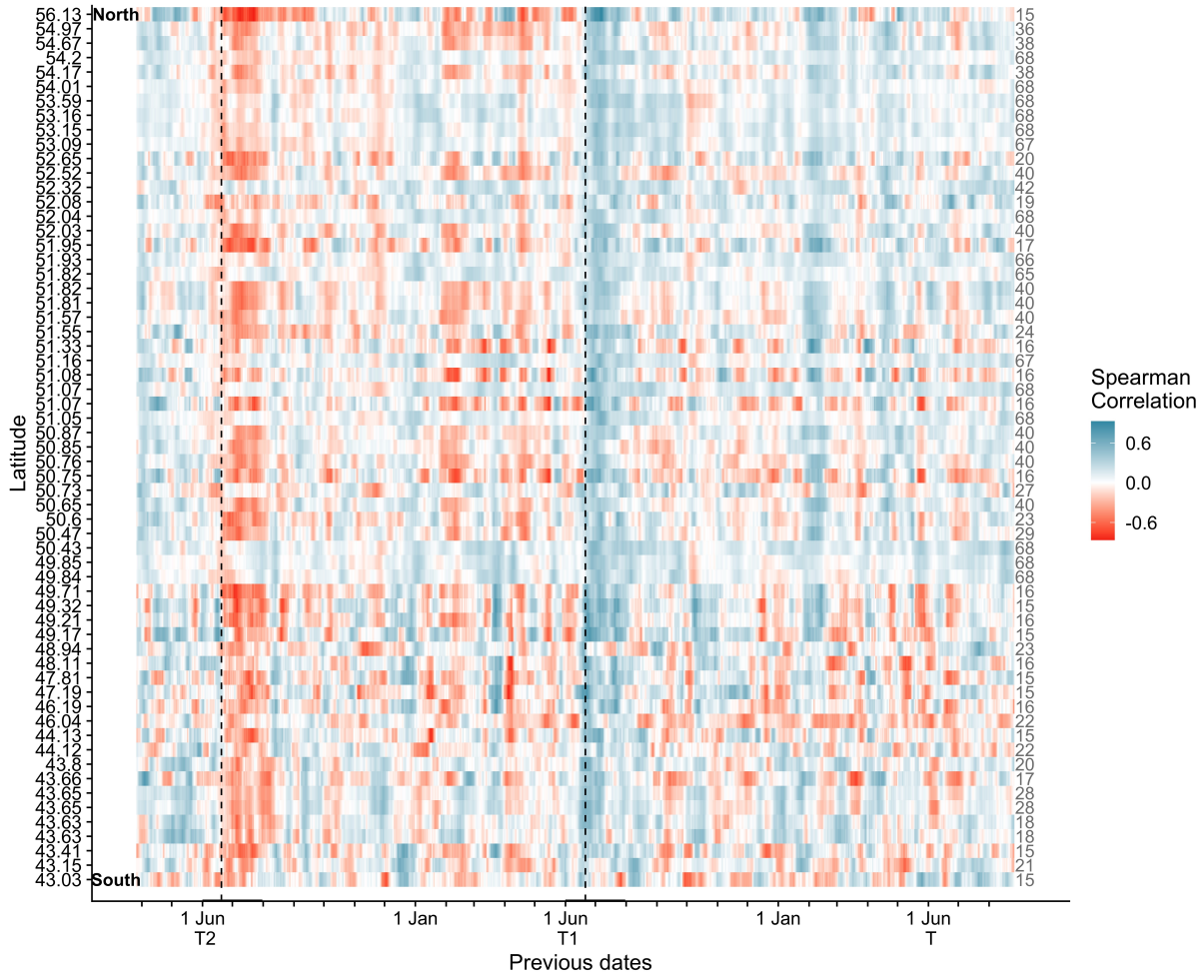

Figure S1: Moving window Spearman correlations between temperature and masting across 61 sites distributed over the European beech range. Black dashed lines indicate the summer solstice (21 June) in each year (one and two years prior to seed fall). Each line represents one site sorted by its latitude (43.03° - 56.13°). The number on the right side of the plot (grey color) indicates site-level sample size (monitoring duration in years). The observations are from the period 1952 - 2019.

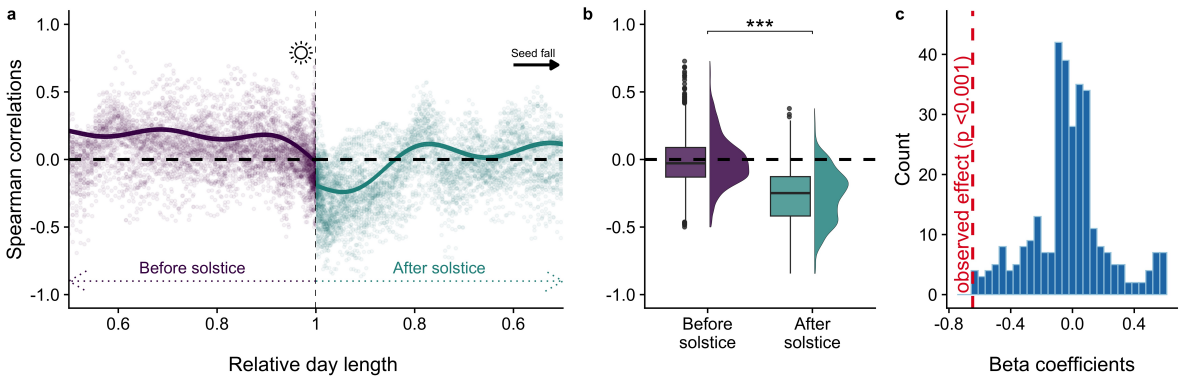

Figure S2: a) Correlations between European beech seed production and temperature at 7-day windows abruptly decrease just after the solstice in year T2. The purple color shows correlations and GAM model prediction for days before the summer solstice and green after the solstice. The prediction lines are based on the GAM model with Spearman correlation coefficients as a response and interaction between relative day length (at the particular time window) and the summer solstice as predictors. Each point is the per site per window correlation coefficient. The predicted correlation at maximum day length is at -0.013 before the solstice and -0.19 after the solstice. The model is summarized in Table S1. b) Correlations before and after the solstice binned into 0.95-1 (maximum) day length before and after the solstice. The *** indicates significance difference between bins tested with GAM ($p < 0.0001$). The median correlation before the solstice is -0.028 and the median correlation after the solstice is -0.25. c) Results of a null model testing whether the abrupt increase in the correlation coefficients (between masting and summer temperatures) is highest at the summer solstice or any other day in the year. Histogram shows the distribution of beta coefficients under the null hypothesis i.e. the before-after difference in correlation coefficients in any other day of the year considered instead of the solstice. The red dashed line shows the observed effect i.e., how correlation coefficients "after solstice" differ as compared to "before solstice". The null model was rejected ($p < 0.001$). All three graphs show the effects for summer T2 (two years before seedfall), effects for summer T1 are presented in Fig. 2.

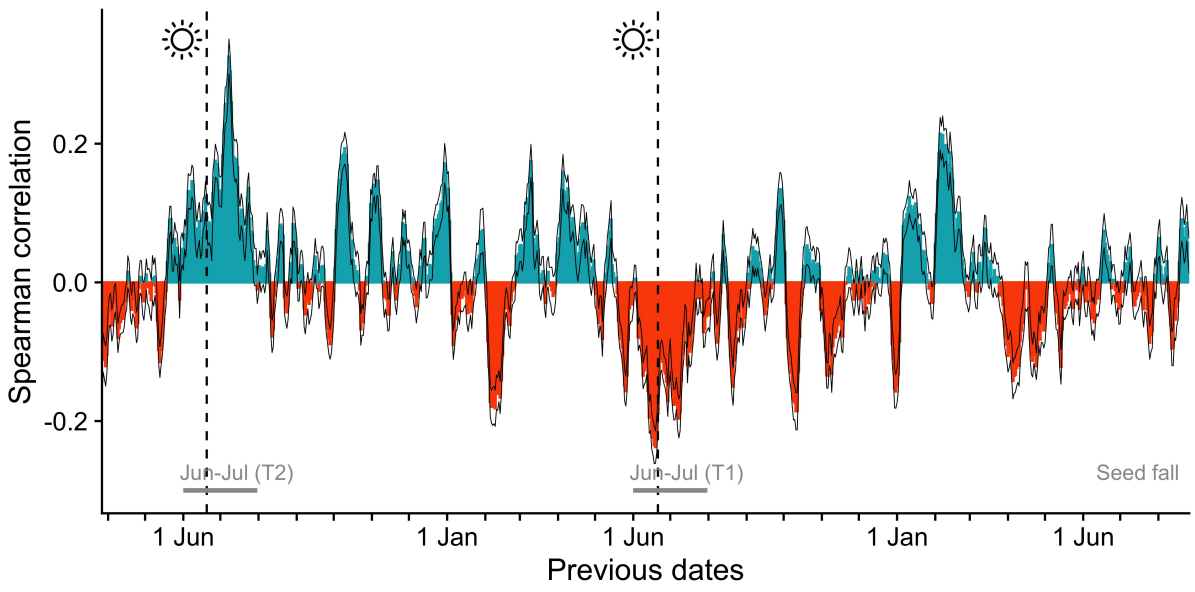

Figure S3: Mean rolling Spearman correlations between precipitation and masting averaged across all 61 sites. The graph shows correlations in two (T2) and one (T1) years before seed production, up until September when seed fall happens. The size of the precipitation window is 7 days, with a 1-day step, and correlations are plotted according to the day of the year at the end of each 7-day window. Black dashed lines close to the sun icon indicate the summer solstice (21st June). Correlations are coded blue for positive, and red for negative. The black solid lines represent the standard error of the correlation coefficients across the sites for each window. Correlations for each site separately are reported in Figure S4.

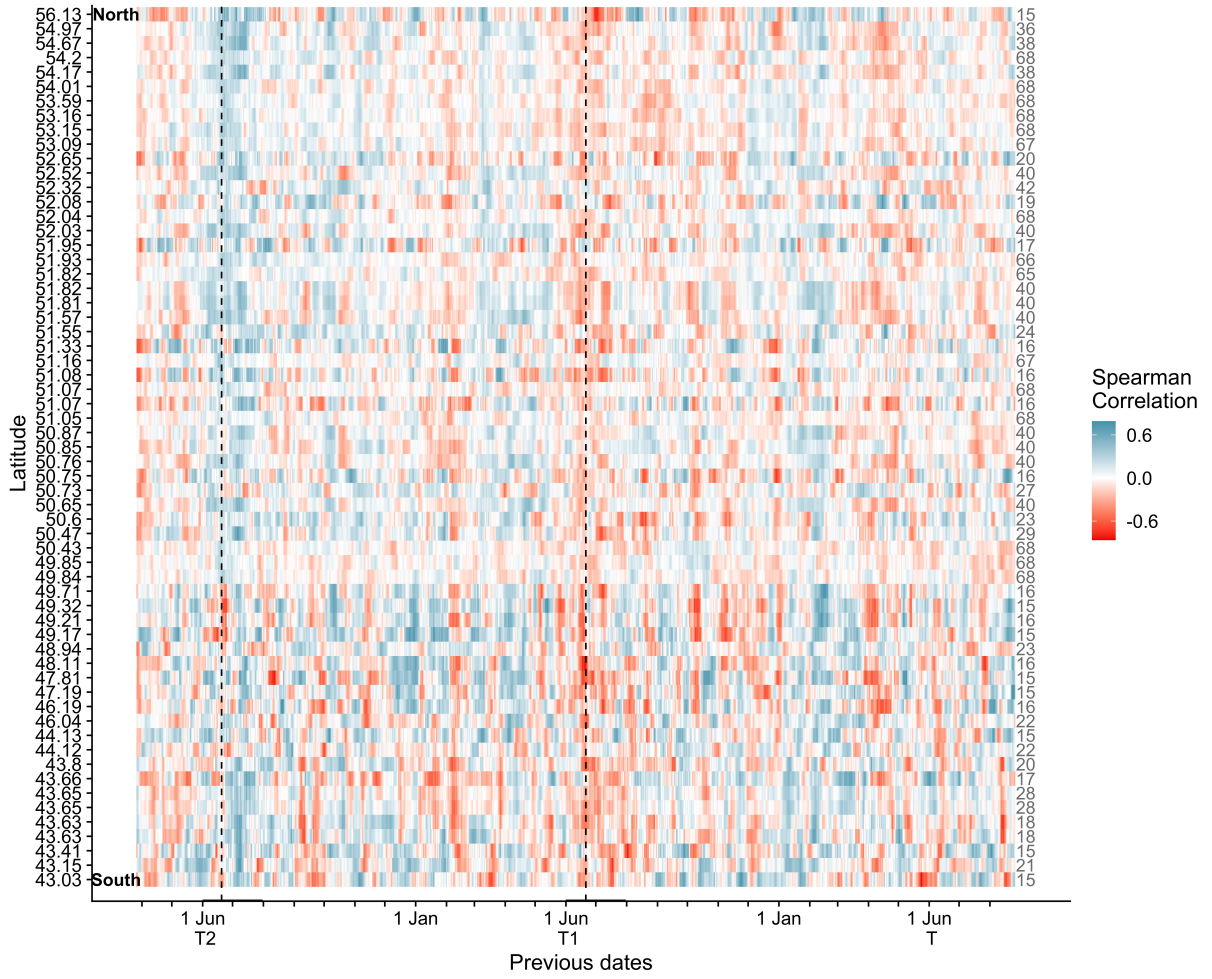

Figure S4: Moving window Spearman correlation between precipitation and masting across 61 sites distributed over the European beech range. Black dashed lines indicate the summer solstice (21 June) in each year (one and two years prior to seed fall). Each line represents one site sorted by its latitude (43.03° - 56.13°). The number on the right side of the plot (grey color) indicates site-level sample size (monitoring duration in years). The observations are from the period 1952 - 2019.

Video: The animation showing the scale of synchrony is provided as a video file. Video shows annual seed production for each site between the years 1995 and 2019, scaled within each site to values between 0 and 1 (to facilitate among-site comparisons). 1995 is shown as the first year as the spatial coverage at that period is highest. Point size is scaled to the size of annual seed production, while the color shows the within-year synchrony among sites. That synchrony is calculated as the inverse coefficient of variation.

Table S1: Summary of generalized additive models (GAM) smooth terms between Spearman correlation coefficient and relative day length for one (T1) and two (T2) years prior seed fall in European beech. Effective degrees of freedom (EDF) represent the complexity of the smooth. Chi-square values indicate the test of significance of smooth terms.

Smooth term	EDF	Chi-squared	p
A) Year T1			
Before solstice	8.99	12.045	< 0.0001
After solstice	8.95	30.095	< 0.0001
Site	59.83	24.134	< 0.0001
B) Year T2			
Before solstice	8.99	7.794	< 0.0001
After solstice	8.99	26.403	< 0.0001
Site	59.46	5.999	< 0.0001